Technical Sciences
Academy of Romania
www.jesi.astr.ro

Journal of Engineering Sciences and Innovation
Volume 6, Issue 2 / 2021, pp. 107-120
http://doi.org/10.56958/jesi.2021.6.2.107

A. Mechanical Engineering

Received ***18 November 2020*** *Accepted* ***17 May 2021***
Received in revised from ***14 January 2021***

Determination of fatigue resistance for steels treated in thermal different ways

TUDORACHE (NISTOR) R.I.[1]*, SAMOILA C.[1,2], URSUTIU D.[1,3]

[1] Transylvania University of Brașov
[2] Romanian Academy of Technical Sciences
[3] Romanian Academy of Scientists

Abstract. In this work is presented an experimental programme for the evaluation of the endurance behaviour of steels which are thermally treated in different ways and the identification of micro-cracks which appear in the material. The fatigue limit was defined as the maximum amplitude of alternating symmetrical stress which steel can endure. In addition to the tests described above. The experimental programme analyses also the change of microstructure under the influence of thermal treatment in view of increasing the working life of materials under stress. The knowledge of the relationships between the structural changes, the internal tensions, the mechanical and physical properties of the material also involve the knowledge of the occurrence of the first nano-cracks.

Key words: fatigue resistance, tensile strengths, symmetrical alternating cycle, microstructure.

Introduction

The main cause for destruction of metallic materials under the influence of mechanical stress is the rupture. Many components of a machine are subject to variable loads during operation. Materials resist to variable stresses less than to the static stresses. The reference value to variable stresses is the fatigue resistance, its determination is regulated by standard SR ISO 1099: 2017" Fatigue test. Controlled axial load method".
The fatigue rupture cannot be identified on time, because it has a progressive nature, the parts works normally until the crack has extended on a certain length, when the final rupture occurs. The fatigue tests are used to make forecasts about

*Correspondence address: roxxannen@yahoo.ro; csam@unitbv.ro; udoru@unitbv.ro

the moment when the materials give in. The tests performed in this work are part of a wider experimental programme in which it is added to the symmetrical alternating stress method and the measurement of Barkhausen noises, which can highlight the moments when nano-cracks appear in the material, the first indicator of the start of rupture process. This work is a first part in which we resort to the classical method of determination of fatigue resistance in order to adjust the thermal treatment processes and to correlate them with the rupture. The research aimed at the following main objectives: determination of the chemical composition of material; determination of micro-hardness; effect of thermal treatment on the fatigue resistance using as method the metallographic analysis; the macroscopic analysis of the rupture surface after the fatigue test.

State of the art

The evaluation by calculation of the lifecycle of a material is important in the decision of selecting the right steel for each application. The good selection of steel involves the selection of an adequate chemical composition and a thermal or thermo-chemical treatment which offers a final homogeneous and flawless microstructure. August Wöhler during over 15 years of experiments made since 1850, on locomotive axles, defined the fundamental laws of fatigue [1]. The fatigue conditions which appear in service are very complex [2]. The initiation of fatigue crack can be appreciated either based on the micro-structural evolution of the material under the action of variable loads or by taking into account the occurrence of nano-micro-crack. In most cases, the initiation of crack is considered the stage during which a structure which does not have flaws and which is subject to variable loads gets micro-cracked and finally will lead to rupture of the structure [3]. Catastrophic accidents were recorded as caused by fatigue, the costliest ones, are the aviation accidents [4]. For these reasons, the study of fatigue resistance behaviour of steels and identification of micro-cracks which appear in the material represents a priority in research. A study conducted by Agius, Kyriakos, Kourousis, Wallbrink, (2018), presents the manufacture of higher quality parts by using the Additive Manufacturing – AM technologies with laser for the purpose of reducing the appearance of micro-cracks [5]. Lashgari, (2020), made investigations on the effect of laser energy density on the microstructure. He used the electronic microscopy (SEM), X-ray diffraction (XRD), Transmission Electronic Microscopy (TEM) in order to obtain quantitative information about the evolution of the microstructure before and after the thermal treatment [6]. Another method of obtaining an increased fatigue resistance, presented by Cong, (2014), consists of melting the steel surface AISI H13 with laser and the powder alloys based on Co and Fe which prevents the propagation of thermal cracks [7]. The microstructures of the areas treated with laser were examined by the electronic microscope. Also, Yadollahi, Shamsaei, Thompson, Elwany, & Bian [8], studied the effect of selective melting by laser of the surface of stainless steel 17-4 PH in order to obtain a higher fatigue resistance. Nezhadfar, [9], investigated the effects of thermal

treatment and roughness of surface on the microstructure and the mechanical properties of stainless steel and noticed that they had a significant effect on the micro-cracks which can appear in the material subject to fatigue test. [10].

Materials and devices

The testing of mechanical characteristics on eprouvettes treated in thermally different ways will highlight the way in which the chemical composition, the micro-alloy elements, the morphology of carbides and the smoothness degree of the structure, influences the mechanical characteristics. The cyclical stresses cause the degradation of material (inter-crystalline and trans-crystalline), which leads to initiation and propagation of crack. The initiation of fatigue crack can have different moments of appearance depending on the micro-structural formation of the material under the action of different regimes of thermal treatments. The purpose of this work was to allow for the correlation between the thermal treatment applied and the rupture.
The eprouvettes for fatigue tests were made according to the provisions of Standard ISO 1099:2017 (fig. 1) and table 1:

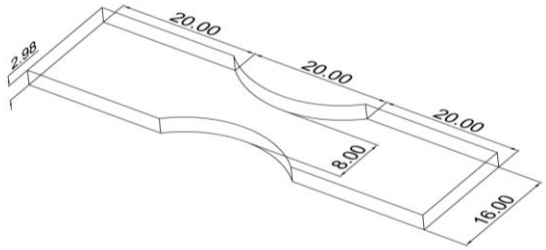

Fig. 1. Sizes of eprouvettes.

The fatigue tests were made in the Company Russenberger Prüfmaschinen AG-Switzerland, on Cracktronik machine at environmental temperature, on which the software Rumul is installed, designed for fatigue tests. A general view of the whole fatigue test system is presented in (Fig. 2) and (Fig.3):

Table 1 Materials subject to testing

Material	**Chemical composition**							
	C	Si	Mn	Cr	Ni	W	Mo	V
C15	0.16	0.03	0.60	-	-	-	-	-
X153CrMoV12	1.59	0.28	0.34	10.9	0.38	0.23	0.93	0.8
X210CrW12	1.92	0.30	0.35	10.8	0.31	0.74	0.22	-
90MnCrV8	0.79	0.33	1.90	0.30	0.11	-	-	0.1
X45NiCrMo4	0.47	0.30	0.31	1.34	4.38	-	0.31	-
C85	0.85	0.35	0.60	0.35	0.38	-	0.06	-
C67	0.68	0.24	0.66	0.20	0.12	-	0.04	-
C 75	0.73	0.22	0.60	0.19	-	-	0.02	-

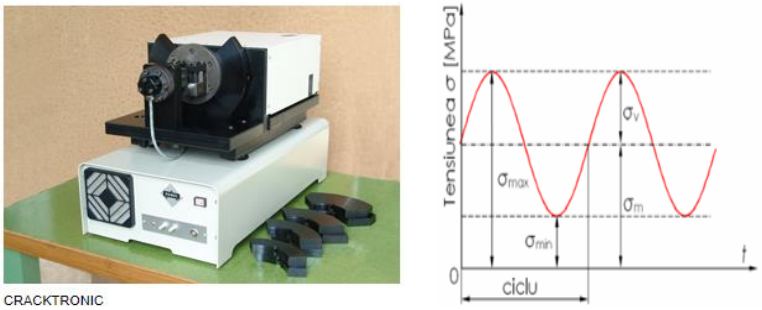

Fig. 2. Fatigue test machine and the stress cycle used.

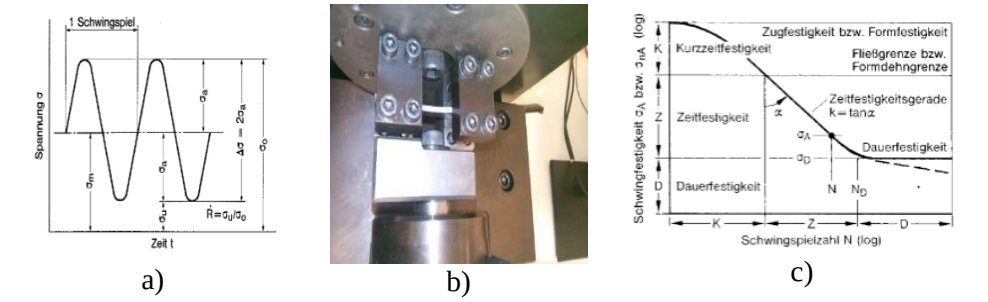

a) b) c)

d) e) f)

g)

Fig. 3. Measurement system and its details a) oscillation period, b) catching of sample, c) Wöhler chart [1], d) measurement system, e) macro-structural analysis, f) inter-crystalline crack, g) fatigue test machine CRAKTRONIK.

Experiment

The eprouvette is caught between two wedge grips and is subject to symmetrical oscillating stress until its rupture. The catching method is presented in Fig. 4.

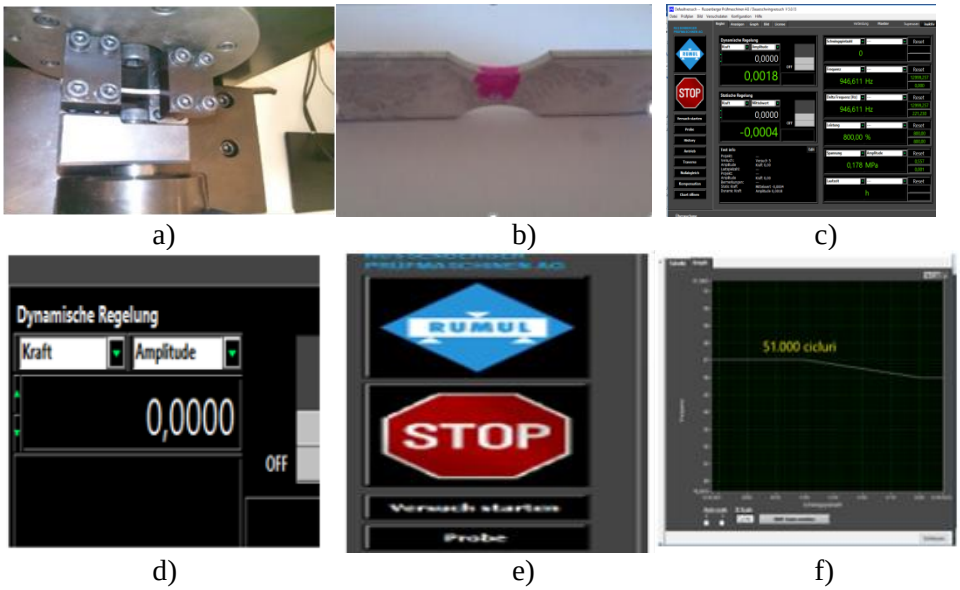

Fig. 4. Catching of eprouvette in the fatigue test machine: a) vibrating wedge grip, b) eprouvette after the fatigue test c) software for fatigue, d) amplitude value, e) start-stop, f) vibration signal.

In these tests, the stress frequencies for all the samples were established at 40 Hz based on information from literature. The initial temperature was about 25°C. The geometric shape of the eprouvette, presented in fig. 1, allows for its rupture in its minimal section.

Are presented the obtained results and tracing of Wöhler curves by fatigue test after a symmetrical alternating cycle, in case of eprouvettes collected from the materials presented in Table 1. In order not to influence the results obtained, we used eprouvettes with the same quality of surface. Were did tests on eight types of materials treated in thermally different ways (see table 2 with the thermal treatments applied) and were used 9 eprouvettes of each quality of experimented steel, in order to allow for a statistical interpretation of results. The macroscopic analysis, respectively the microscopic analysis, was performed by the optical microscope Keyence from the equipment of ”Härterei Reese” Laboratory Brackenheim.

For determination of fatigue limit, was traced the endurance curve σ_{adm}-N in which σ_{adm} represents the maximal stress tension, and N is the number of stress cycles until rupture. For each stress level were used nine eprouvettes, the fatigue test order was from high tensions to low tensions, the first fatigue test step was at $\sigma_{adm} = 0.6\ Rm$.

where: σ_{adm} -maximum tension introduced in eprouvette;
Rm- mechanical resistance of material.
The tests will continue until was reach that at least one eprouvette does not break. With the values σ_{adm}-*N* were trace a curve just like in Fig. 5 (Wöhler curve). The estimation of lifecycle by using Wöhler curve gives results quite close to the number of cycles set out to assure a good resistance of the material in exploitation.

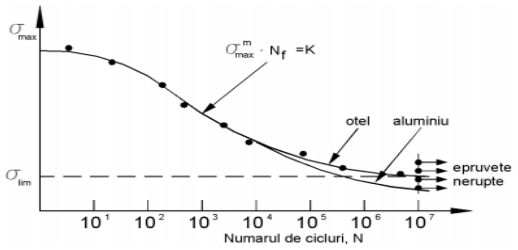

Fig. 5. Fatigue curve or Wöhler curve.

The eprouvettes subject to fatigue test were made in the company Matthias Meidlinger GmbH-Brackenheim. Their final roughness was between 0.03-0.14 µm. A low roughness of the eprouvette surface is important, because the variable loads usually activate surface defects. The thermal treatment, respectively the metallographic check of eprouvettes was made in the company Reese Härterei from Brackenheim. In Table 2 are presented the results of fatigue tests in different variants of thermal treatment of a varied range of steels. The data are for guidance because the thermal treatment can substantially influence the fatigue resistance [11].

Table 2. Thermal treatment for eprouvettes subject to fatigue test.

Material	Thermal treatment [1]			Fatigue resistance σ_{-1} (MPa)	Fracture strength Rm (MPa)
	Temperature conditions		Cooling environment		
C75	C 840	R 540	oil	471.75	1095
C15	Cem 940 C 850	R 220	oil	598.5	1290
x45CrNiMo4	C 820	R 580	oil	618	1320
C 67	C 820	R 540	oil	510.75	1155
X 153CrMoV12	C 1040	R 610	Nitrogen	610	1700
C85	C 820	R 540	oil	660	1385
90MnCrV8	C 820	R 500	oil	638	1350
210CrW12	C 1040	R 610	Nitrogen	563	1665

[1] Were used the abbreviations: C_{em} - cementation C - tempering, R – high return, r – low return, σ_{-1} fatigue resistance. Rm – fracture strength of material, Rm or σ_r (Rm in SR EN 10 0002:1;1994).

The metallographic analysis highlighted a very smooth structure for the materials with high content of manganese (90MnCrV8) and high content of nickel

(x45NiCrMo4). According to the theory by association of Ni in steels with Cr, W, Mo are obtained superior mechanical properties.

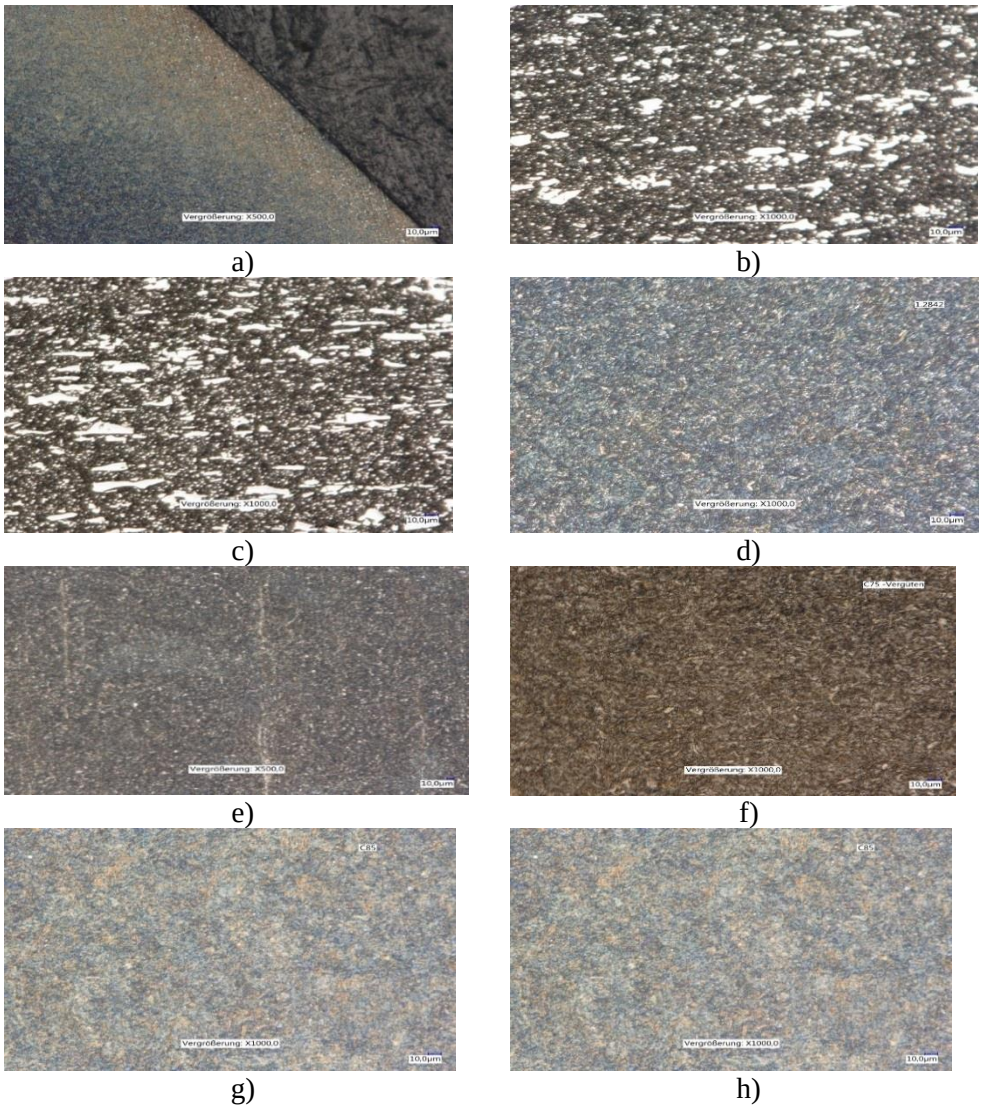

Fig. 6. Metallographic structures after the thermal treatment a) represents the material C15 after the thermo-chemical treatment of cementation; b) x 153CrMoV12 after the thermal treatment of tempering in vacuum at temperature of 1040^0C and return to 610^0C; c) 210 CrW12 after the thermal treatment of tempering in vacuum at temperature of 1040^0C and return to 610^0C; d) 90MnCrV8 after the thermal treatment of tempering with cooling in oil and return to 500^0C; e) x 45CrNiMo4 after the thermal treatment of tempering and return to 580^0 C; f) C 75 after the thermal treatment of improvement; g) C 85 after the thermal treatment of improvement; h) C 67 after the thermal treatment of improvement.

Determination of fatigue resistance was made as follows:
The eprouvette tests were made in several steps of maximum tension. The eprouvettes were loaded with descending loads. The intervals between steps were 30 MPa.
Step I: The first eprouvette tested is loaded with a force which induces a tension $\sigma_{adm} = \sigma_1 = 0{,}6\ \sigma_r$, noting the number of cycles with (N_1),
Step II: The second eprouvette from the batch is loaded with a lower load than the first one, so that $\sigma_2 = \sigma_1 - 30$ MPa and we note the number of cycles until the rupture N_2.
Step III: The next eprouvette tested $\sigma_3 = \sigma_2 - 30$ MPa noting the number of cycles until rupture N_3.
Was continued the fatigue tests until were reach that at least one eprouvette does not break. The number of cycles N_0 after which the eprouvettes do not break can have values between $2 \times 10^6 - 2 \times 10^7$. Depending on the number of eprouvettes can be tested one or more eprouvettes at each tension step. Depending on the sizes of eprouvette and σ_{adm} were calculated the amplitude by which the eprouvettes are tested. The repeated stresses of the material lead to reduction of its resistance. This reduction is influenced by: N – Number of cycles applied, σ_{adm} – maximum tension introduced in eprouvette, sizes in SI, *M* – amplitude of cycle. In the calculation of resistance module, were consider that the axes *y* and *z* are main central axes. Geometric sizes: [2]

$$Wz = \frac{I_z}{y_{max}} \text{ and } Wy = \frac{I_y}{z_{max}} \text{ [mm]} \quad (1)$$

Are called resistance modules compared to axis *z*, respectively *y*, where I_z and I_y represent the axial inertia moment.
In the formulas above y_{max}, respectively z_{max} are the distances of the furthest point of section compared to axis *Oz*, respectively *Oy*.
In case of rectangular sections, the axial resistance modules result from:

$$Wz = \frac{I_z}{y_{max}} = \frac{b*h^3}{12} \frac{2}{h} = \frac{bh^2}{6} \text{ [mm]} \quad (2)$$

$$Wy = \frac{I_y}{z_{max}} = \frac{b^3h}{12} \frac{2}{b} = \frac{b^2h}{6} \text{ [mm]} \quad (3)$$

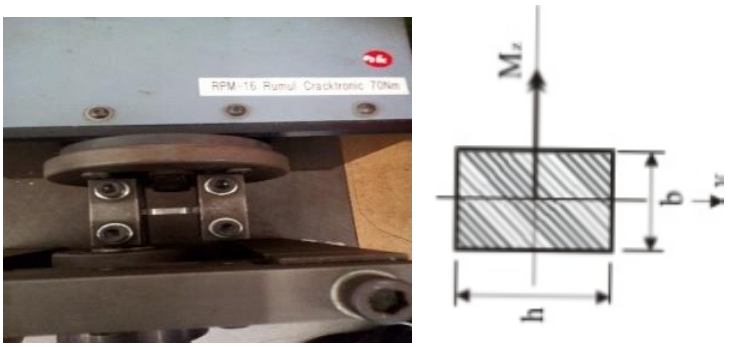

Fig. 7. Positioning of eprouvette in the fatigue testing machine.

In case of tested eprouvettes and the catching method of eprouvette in the setting of cycle amplitude were used the following formulas:

$$M = \sigma_{adm} \cdot W_y \text{ [Nm]}$$

$$M = \frac{hb^2}{6}\sigma_{adm} \text{ [Nm]} \quad (4)$$

W_y – is called axial resistance module;

σ_{adm} – the maximum tension introduced in eprouvette in the section which will break.

For the steels in which mechanical resistance, $R_m < 1400$ MPa fatigue limit (σ_{adm}) was chosen as 0.65 R_m, and for steels with mechanical resistance $R_m > 1400$ MPa were chosed 0.5 R_m. Based on the recommendations from literature $\sigma_{adm} \approx$ 0.35 up to 0.65 R_m.

The other sizes included in formula 4 have the values:

h = 2.98 mm (measured on each eprouvette);

b = 8 mm (measured on each eprouvette).

The results obtained after the tests are presented, with the specification of type and size of eprouvettes, the loading order of each eprouvette (table 3), characteristic of stress cycle (tension σ_{adm} - amplitude M), the number of cycles until the rupture and the observations after the tested examinations. (Table 4).

Table 3 Calculation of admissible tension for the materials studied

Mat.	C75		C15		X45NiCrMo4		C67		X153CrMoV12		C85		90MnCrV8		210CrW12	
Rm	1095		1290		1320		1155		1700		1385		1350		1665	
	σ_{adm}	M	σ_{adm}	M	σ_{adm}	M	σ_{adm}	M	σ_{adm}	M	σ_{adm}	M	σ_{adm}	M	σ_{adm}	M
Tr.1	711.75	23	838.5	27	858	27	750.75	24	850	27	900	29	878	28	833	26
Tr.2	681.75	22	808.5	26	828	26	720.75	23	820	26	870	28	848	27	803	25
Tr.3	651.75	21	778.5	25	798	25	690.75	22	790	25	840	27	818	26	773	24
Tr.4	621.75	20	748.5	24	768	24	660.75	21	760	24	810	26	788	25	743	23
Tr.5	591.75	19	718.5	23	738	23	630.75	20	730	23	780	25	758	24	713	22
Tr.6	561.75	18	688.5	22	708	22	600.75	19	700	22	750	24	728	23	683	21
Tr.7	531.75	17	658.5	21	678	21	570.75	18	670	21	720	23	698	22	653	20
Tr.8	501.75	16	628.5	20	648	20	540.75	17	640	20	690	22	668	21	623	19
Tr.9	471.75	15	598.5	19	618	19	510.75	16	610	19	660	21	638	20	593	18

Table 4. Results obtained for fatigue resistance.

Material	h [mm]	b [mm]	HRC	Rm [MPa]	∂ad [MPa]	M (Nm)	Lifecycle (number of cycles)
C75	2.98	8	34.36	1095	471.75	15	5 907 813
C15	2.98	8	40.8	1290	598.5	19	224.159
X45NiCrMo4	2.98	8	41.45	1320	618	19	174 521
C67	2.98	8	36.51	1155	510.75	16	145 870
X153CrMoV12	2.98	8	49.96	1700	610	19	140 558
C85	2.98	8	44	1385	660	21	115 379
90MnCrV8	2.98	8	41.9	1350	638	20	53 694
210CrW12	2.98	8	50	1665	593	18	16 744

In table 4 were given the result for σ_{adm} in the last stress step.

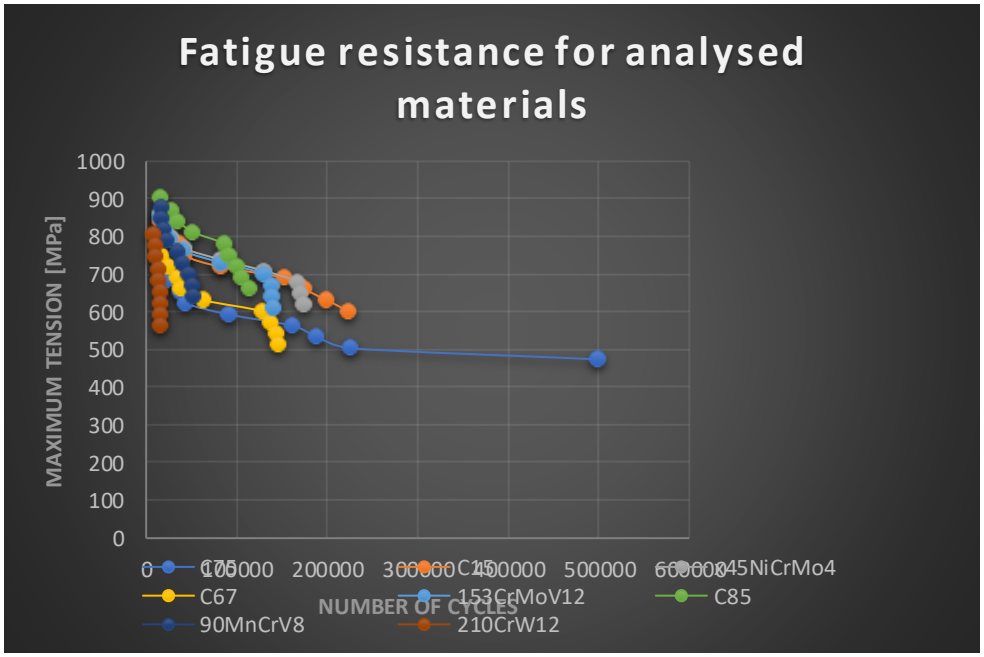

Fig. 8. Wöhler diagrams for the studied materials.

Since 1850 Wöhler highlighted that for a certain maximum tension, the number of cycles until rupture decreases if the tension variation increases [1]. Therefore, from Wöhler diagrams (Fig. 8) for the studied materials we can see that as the amplitude of stress cycles increases, the number of stress cycles decreases, respectively the working life of material. From the tests performed, where the admissible tension has the minimal value of 510.75 MPa and maximum value of 660 MPa, it results a number of cycles until yield N between 1.45×10^5 and 1.1×10^5. A tension amplitude of $\sigma_{adm} = 471$ MPa leads to 6×10^6 cycles without yield. As the amplitude increases, the working life of material decreases.

By Barkhausen noises we want to identify the moment when the first nano-crack appears. The initiation of the crack could be identified by the Rumul Software specialised for this purpose. Therefore, after the application of a sufficient number of stress cycles, in the material successive structural changes are made, which lead to the appearance of nano-cracks. In order to be able to make a correct analysis of the moment when nonconformities appear in the material, we examined the activity of signals which have as coordinates the frequency and number of cycles.

By measurements (Fig. 9) we recorded the moment when nonconformities appear in the material, which lead to initiation of crack. According to the diagrams from Fig. 9 (a, b, c, d, e and f) we can notice a constant of value up to a certain point, then follows a linear decrease. This decrease of value is due to the appearance of nano-cracks at the level of crystalline network. In Fig. 9 (g and h) we can notice a

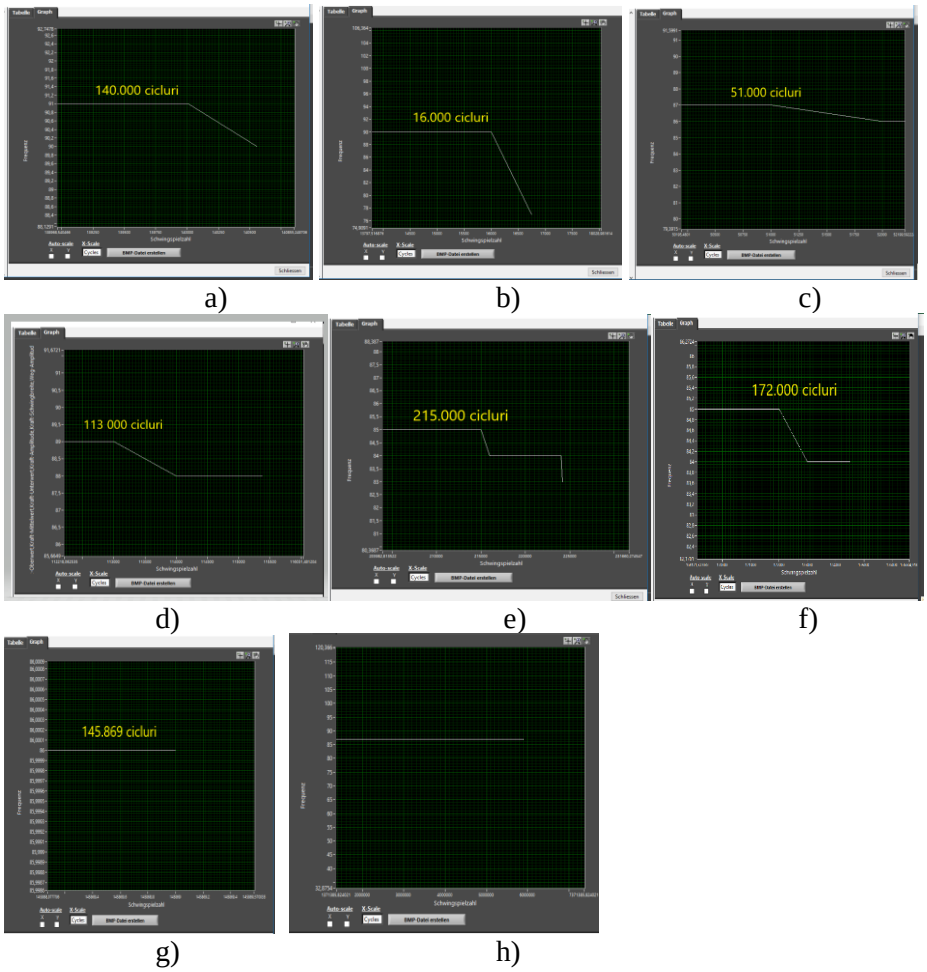

Fig. 9. Moment of appearance of the first nano-crack in the material a) For the material x153CrMoV12 the moment of appearance of the first nano-crack was at 140,000 cycles; b) For the material 210CrW12 the moment of appearance of the first nano-crack was at 16,000 cycles; c) For the material 90MnCrV8 the moment of appearance of the first nano-crack was at 51,000 cycles; d) For the material C 85 the moment of appearance of the first nano-crack was at 113,000 cycles; e) For the material C15 the moment of appearance of the first nano-crack was at 215,000 cycles; f) For the material x45NiCrMo the moment of appearance of the first nano-crack was at 172,000 cycles; g) For the material C67 the moment of appearance of the first nano-crack was at 145,869 cycles; h) For the material C75 we did not record the appearance of nano-crack. The material resisted 5 907 813 without breaking.

constant of value. In case of g, the material C 67 worked for 145,869 cycles then it broke. You can see from the diagram that the material broke without having nano-cracks, which shows a high purity of material, respectively a mechanical processing without having introduced internal tensions in the material.

And in case of material C 75 from Fig. 9.h we notice a constant of value without the appearance of nano-cracks or rupture. It worked until 5 907 813 cycles without

rupture. For each material we used a different amplitude, depending on the hardness of material subject to testing. The amplitude value can be found in Table 4. Thus, the material which recorded a faster appearance of nano-crack was the material 210CrW12 in which we used an amplitude of 18Nm and in steel C75 which worked without breaking we used an amplitude of 15Nm. If we compare the hardness of the two materials 50 HRC for the material 210CrW12 in which we recorded the first appearance of nano-crack and 34,36 HRC for the material C 75 which did not break, we can draw the conclusion that the materials with high hardness record a faster appearance of nano-cracks in the crystalline network compared to those which have a low hardness.

Table 5. Initiation and propagation of crack in experimented steels.

Material	**Initiation of crack %**	**Propagation %**
X153CrMo V12	99,6	0,4
210CrW12	95,5	4,5
90MnCrV8	94,9	5,1
C85	97,9	2,1
C15	95,9	4,1
X 45NiCrMo	98,6	1,4
C 67	99,9	0,1
C 75	Without crack	Without rupture

In the table 5 (above) you can see that the initiation of crack requires about 97.5% of the testing period and the propagation 2.5%. We exemplified below a few important results of the specialised literature in the field of fatigue resistance compared to the results obtained on the materials experimented in this research. A recent work [12] analysed the problem of correlations between the characteristics of stretch resistance and fatigue resistance at stresses with symmetrical alternating cycle in case of a wide range of steels with fracture resistance between 370 and 2330 N/mm^2. The formula which best reflects the results of tests done is:

$$\sigma_{adm} = 0{,}37 \cdot R_m + 75 \quad (5)$$

The results obtained with the Buthod formula $\sigma_{adm} = 0{,}37 \cdot R_m + 75$ and those obtained by experimental path with the formula $\sigma_{adm} = 0{,}65 \cdot R_m$ are illustrated in Table 6. We can see that the results obtained with different formulas are comparable.

Table 6. Difference between the theoretical fatigue resistance σ_{-1} and σ_{-1} experimental fatigue resistance.

Material	σ_{adm} **Buthod** N/mm^2	σ_{adm} **experimental** N/mm^2
C75	480	472
C15	552	598.5
X45NiCrMo4	563	618
C67	502	510
X153CrMoV12	704	610
C85	588	660
90MnCrV8	574	638
210CrW12	691	593

Many authors tried to connect the fatigue limit to the mechanical characteristics and especially to the stretch resistance Rm (Mpa), to yield limit $R_{p0,2}$ [N/mm^2], to elongation at rupture A and rupture constriction, expressed in percentages, Z and different formulas are proposed [3].

Discussions and appreciations

The investigation of fatigue resistance in laboratory has an important role in the selection of material and the thermal and thermo-chemical treatment processes. The appreciation of the behaviour of fatigue resistance of materials was made based on the Wöhler curves and the micro-structural investigations and based on the mechanical characteristics of the material. Based on the research carried out, we could analyse by comparison the effect of thermal treatments applied to the behaviour of fracture resistance of materials studied. From table 2 you can see that the most favourable values for fatigue resistance are offered by the thermal treatment of improvement applied to the material C75 with sorbitic structure and a hardness of 1095 MPa (34.36 HRC), and the most unfavourable values for fatigue resistance are offered by the thermal tempering treatment applied to the material 210CrW12 with martensitic structure with uneven carbides and a hardness of 1665 MPa (50 HRC). A low hardness of the material in connection with a smooth metallographic structure which is obtained after the improvement treatment justifies the increase of fatigue resistance of the material.

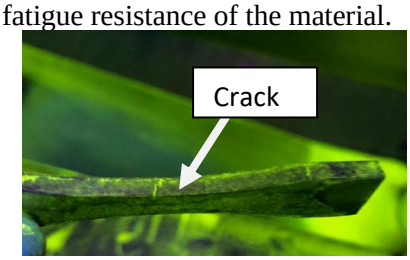

Fig. 10. Macroscopic and microscopic check for experimented steels.
Identification of crack by magnetic powders.

With the macroscopic analysis at a 100x zoom we identified the cracked area following the fatigue resistance, area which was later subject to examination with magnetic powders. Ni and Mo from the structure of steel x45CrNiMo4 made that it resisted to fatigue with a number of cycles N of 174521. We can see that the carburized steel with a diffusion layer of 0.54-0.57 mm resisted for 224159 cycles; this increase is due to the thermochemical treatment to which the eprouvette was subjected. If we relate to the carbon from the chemical composition, we can draw the conclusion that the steels with C over 0.9% resist less to fatigue. We can see that the fatigue resistance property has a minimal value in case of x210CrW12 and maximum value in case of steel C75, so it is inversely proportional to the hardness of material influenced by the content of C and by the alloying degree. We can see that the steel 210CrW12 with most carbides (carbides of Cr and W) resisted the least to fatigue, because after a number of 16,744 cycles, the rupture was caused. We can also see that because of carbides from the structure and the high content of C, the rupture was completely caused unlike the other steels where only the initiation of crack was caused.

a) b)

Fig. 11. Macroscopic check for the steel with low fracture resistance, respectively high fracture resistance: a) represents the eprouvette made of material x210CrW12; b) represents the eprouvette made of material C15.

Conclusions

In this work we analysed the way in which the application of different types of thermal treatments influences the appearance of micro-nano-cracks in the material. We developed a calculation algorithm for shortening the fatigue testing time without influencing the final results which have three variables: - size of eprouvette, - amplitude, - mechanical characteristics of the material depending on its metallographic structure. The experimental results were checked by the theoretical and practical comparative analysis from the specialised literature.

By the analysis of frequency diagrams by using the Barkhausen noises, we identified nano-cracks which appeared during the experiments made for testing the fatigue resistance as starting point of final rupture.

References

[1] Oliviu, R., Teodorescu M., Lascu N., *Oboseala metalelor. Baze de calcul*, vol. 1, Ed. Tehnică, Bucureti, 1992.

[2] Geru N., *Teoria structurală a proprietăţilor metalelor*, Editura Didactică şi Pedagogică, Bucureşti, 1980.

[3] Dumitru I., Faur N., *Bazele teoretice în oboseala materialelor, Mecanica Ruperii, Materiale compozite si Metode Numerice*, Editura Tehnică, 1997.

[4] Harold B., *Nondestructive Testing Standards- A Review*, in ASTM Special Technical Publication 624, American Society for Testing and Materials, Philadelphia, 1977.

[5] Agius, D., Kourousis I., Wallbrink C., *A review of the as-built SLM Ti-6Al-4V mechanical properties towards achieving fatigue resistant designs*, Metals, 2018.

[6] Lashgari, H. R. et al. *Microstructure, post thermal treatment response, and tribological properties of 3D printed* 17-4 PH stainless steel, Wear, 2020.

[7] Cong, Dalong, et al., *Thermal fatigue resistance of hot work die steel repaired by partial laser surface remelting and alloying process*. Optics and Lasers in Engineering, **54**, p. 55-61, 2014.

[8] Yadollahi, A., Shamsaei, N., Thompson, S. M., Elwany, A. & Bian, L., *Effects of building orientation and heat treatment on fatigue behavior of selective laser melted 17-4 PH stainless steel*, International Journal of Fatigue, **94**, 2017, p. 218-235.

[9] Nezhadfar, P. D. et al., *Fatigue behavior of additively manufactured 17-4 PH stainless steel:Synergistic effects of surface roughness and heat treatment*, International Journal of Fatigue, 2019.

[10] Santos, L. M. S. et al., *Effect of heat treatment on the fatigue crack growth behaviour in additive manufactured AISI 18Ni300 steel*, Theoretical and Applied Fracture Mechanics, 2019.

[11] A.P Guliaev, *Metalurgie fizica*, Editura tehnica, 1954.

[12] Buthod, H şi Lieurade, H.P., *Influence des propriétés mécaniques sur les caractéristiques d'endurance en flexion d'une gamme étendue d'aciers**, Rev. Met. Paris Rev. Met. Paris, **83**, Number 6, Juin 1986.